Isotropically conducting (hidden) quantum Hall stripe phases in a two-dimensional electron gas

Yi Huang (□□), M. Sammon, M. A. Zudov, and B. I. Shklovskii

Phys. Rev. B **101**, 161302 — Published 20 April 2020

DOI: 10.1103/PhysRevB.101.161302

Isotropically conducting (hidden) quantum Hall stripe phases in a two-dimensional electron gas

Yi Huang (黄奕),* M. Sammon, M. A. Zudov, and B. I. Shklovskii
School of Physics and Astronomy, University of Minnesota, Minneapolis, Minnesota 55455, USA
(Received March 30, 2020)

Quantum Hall stripe (QHS) phases, predicted by the Hartree-Fock theory, are manifested in GaAs-based two-dimensional electron gases as giant resistance anisotropies. Here, we predict a "hidden" QHS phase which exhibits *isotropic* resistivity whose value, determined by the density of states of QHS, is independent of the Landau index N and is inversely proportional to the Drude conductivity at zero magnetic field. At high enough N, this phase yields to an Ando-Unemura/Coleridge-Zawadski-Sachrajda phases in which the resistivity is proportional to $1/N$ and to the ratio of quantum and transport lifetimes. Experimental observation of this border can provide a new way to obtain quantum relaxation time.

Quantum Hall stripe (QHS) phases in spin-resolved Landau levels (LLs) near half-integer filling factors $\nu = 9/2, 11/2, 13/2, ...$, were predicted by the Hartree-Fock (HF) theory [1–3]. These phases consist of alternating stripes with filling factors $\nu \pm 1/2$, which, at exactly half-filling, both have the width $\Lambda/2 \simeq 1.42\,R_c$ [1, 2, 4, 5], where R_c is the cyclotron radius (see Figure 1). QHSs are formed due to a repulsive box-like interaction of electrons having ring-like wave functions. Such an unusual interaction leads to an energy gain when electrons occupy the nearest states within the same stripe and avoid interacting with electrons in neighboring stripes. The self-consistent HF theory is valid at LL indices $N \gg 1$, when $R_c = l_B(2N+1)^{1/2} \gg l_B$, where $l_B = (c\hbar/eB)^{1/2}$ is the magnetic length, a measure of quantum fluctuations of an electron's cyclotron orbit center, and B is the magnetic field. These fluctuations play a minor role even at $N = 2$, and QHSs determine the ground state for all $\nu \geq 9/2$ [2, 4, 5].

QHSs were confirmed by the discovery of dramatic resistance anisotropies in two-dimensional electron gases in GaAs/AlGaAs heterostructures [6, 7]. These anisotropies emerge because the diffusion mechanisms along and perpendicular to the stripes are different [8]. In the stripe direction ($\hat{y}$) electrons drift along the stripe edge in the internal electric field $\mathbf{E}$ until they are scattered to an adjacent stripe edge by impurities. If such scattering is weak, this mechanism leads to a large diffusion coefficient in the $\hat{y}$ direction (large conductivity σ_{yy}, large resistivity ρ_{xx}) and a small diffusion coefficient in the orthogonal ($\hat{x}$) direction (small σ_{xx}, small ρ_{yy}). As a result [9], if N is not too large,

$$\frac{\rho_{xx}}{\rho_{yy}} \simeq \left(\frac{\tilde{\sigma}_0}{8\gamma\alpha^2 N^2}\right)^2 \gg 1\,, \qquad (1)$$

where $\tilde{\sigma}_0 = n_e h\tau/m^\star$ is the Drude conductivity at $B = 0$ in units of e^2/h, n_e is the electron density, τ is the momentum relaxation time, $m^\star$ is the electron effective mass, and γ is a discussed below numerical factor depending on the nature of scattering. To derive Eq. (1) we used the HF potential, shown in Figure 1(a), with the amplitude $\Gamma_s \simeq 0.4\,\hbar\omega_c/\alpha$, where ω_c is the cyclotron frequency, and $\alpha \simeq 18$ is the ratio of the density of states (DOS) in the middle of a spin split LL to that without magnetic field, but per spin [10]. In Ref. 9 we showed that Eq. (1) agrees well with the data from high mobility samples.

At large enough N, Eq. (1) predicts that the anisotropy of resistivity vanishes. In this Rapid Communication we theoretically study $\rho(N, \tilde{\sigma}_0)$ at half-integer ν in emerging at such N isotropic phase. Our results are summarized in the "phase diagram" of $\tilde{\rho} \equiv (e^2/h)\rho(N, \tilde{\sigma}_0)$ depicted in Figure 2. In the top-left corner it shows the anisotropic QHS phase, discussed above. The remaining three phases are isotropic. The Ando-Unemura (AU) phase [11] and the Coleridge-Zawadzki-

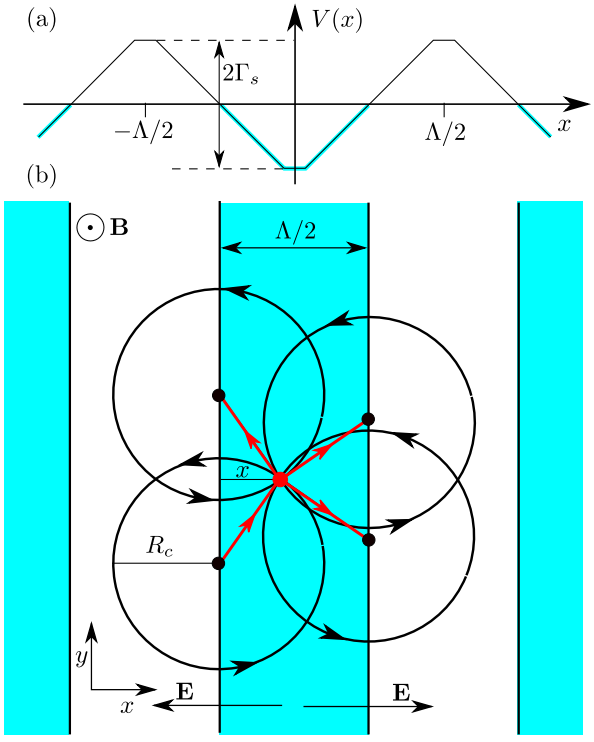

Figure 1. (a) HF potential energy $V(x)$ responsible for QHS formation [2] at half-integer ν. The slope of $V(x)$ determines the internal electric field $\mathbf{E}$. States shown by thick (cyan) lines are populated by electrons. Λ is the $V(x)$ period and Γ_s is its amplitude. (b) Impurity scattering dominated hopping transport in hidden QHS phase in the quasi-classical ($N \gg 1$) limit. An electron with the guiding center (black dot) at the lower left edge of the central electron stripe is scattered off an impurity (red dot) at the distance x from its edge. Three possible hops of the guiding center are shown by red arrows.

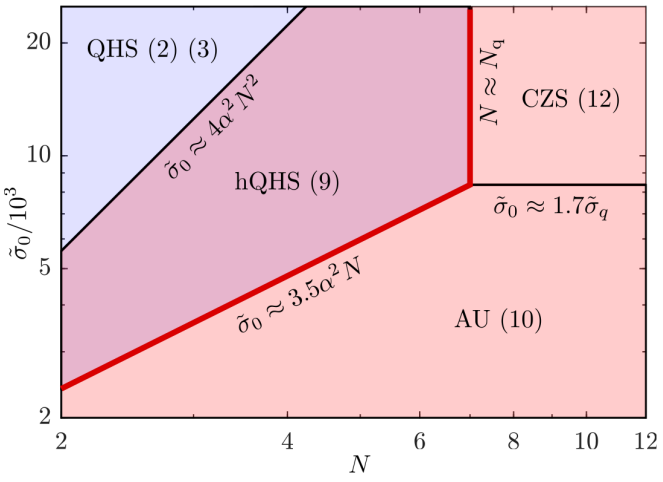

Figure 2. Phase diagram for $\tilde{\rho}$ in the $(N, \tilde{\sigma}_0)$-plane. In the QHS phase $\tilde{\rho}_{xx} \gg \tilde{\rho}_{yy}$, while in the hQHS, AU, and CZS phases $\tilde{\rho}_{xx} = \tilde{\rho}_{yy}$. Numbers in parentheses label equations for $\tilde{\rho}$ in corresponding phases. Thick boundaries mark destruction of stripe phases where $\Gamma_i \sim \Gamma_s$. N_q and $\tilde{\sigma}_q$ are given by Eqs. (13) and (14), respectively [13].

Sachrajda (CZS) phase [12] correspond to a regime in which the LL width due to impurity scattering Γ_i dwarfs the amplitude of the HF potential of stripes Γ_s so that stripes are destroyed by disorder and, as a result, in both phases $\tilde{\rho} \propto 1/N$. However, $\tilde{\rho}$ in these two phases differ by the ratio τ/τ_q of momentum and quantum relaxation times; the AU phase occurs in low-mobility samples, in which the short range scattering determines both scattering times ($\tau/\tau_q = 1$), while the CZS phase corresponds to high mobility samples in which scattering on Coulomb impurities leads to $\tau/\tau_q \gg 1$.

On the other hand, to the best of our knowledge, the third isotropic phase, located between the QHS and the AU/CZS phases, has not been discussed in the literature. In this phase $\Gamma_s \gg \Gamma_i$ and electrons still form stripes, but there is no significant anisotropy of the resistivity. This happens because the drift along $\hat{y}$ direction gives smaller contribution to the conductivity than the impurity scattering, which leads to hops of the cyclotron center in all directions at the distance of the order of R_c, see Figure 1 (b). Although, generally speaking, this is not enough to make conductivity of an anisotropic system isotropic we will show below that for QHS with period $\Lambda = 2.84\, R_c$ and large N resistivity anisotropy does not exceed a few percents. Therefore, in a semi-quantitative theory, we treat this phase as an isotropic one and call it the "hidden QHS" (hQHS) phase. Like in the QHS phase, the density of states in the hQHS phase is determined by the HF potential $V(x)$ and, as a result, $\tilde{\rho}(N, \tilde{\sigma}_0)$ in the hQHS phase is independent of N.

Let us now derive the borders of all four phases and the expressions for $\tilde{\rho}(N, \tilde{\sigma}_0)$ for a series of samples with the roughly the same density ($n_e \simeq 3 \times 10^{11}$ cm^{-2}) and widely varying (from $\sim 10^6$ to $\sim 10^7$ cm^{2}V^{-1}s^{-1}) mobility, which are made of high mobility GaAs quantum wells by replacing a small fraction x of Ga atoms with Al [14]. In these samples, the short-range Al impurities significantly affect the momentum relaxation rate τ^{-1} which increases linearly with x [14]. We further assume that the quantum scattering rate τ_q^{-1} is determined by scattering on Coulomb background impurities and remote donors at small x (large $\tilde{\sigma}_0$), and therefore is independent on x, but eventually approaches τ^{-1} at larger x (small $\tilde{\sigma}_0$). We show below that for such samples $\gamma \simeq 0.5$.

QHS phase. Combining Eq. (1) with $\gamma \simeq 0.5$ and Eq. (36) of Ref. 8, $(\tilde{\rho}_{xx}\tilde{\rho}_{yy})^{1/2} \simeq 1/8N^2$, we find

$$\tilde{\rho}_{xx} \simeq \frac{\tilde{\sigma}_0}{32\alpha^2 N^4}\,, \tag{2}$$

$$\tilde{\rho}_{yy} \simeq \frac{\alpha^2}{2\tilde{\sigma}_0}\,. \tag{3}$$

For a given $\tilde{\sigma}_0$ the "hard" $\tilde{\rho}_{xx}$ scales with N^{-4} whereas the "easy" $\tilde{\rho}_{yy}$ is N-independent. The border between the QHS and hQHS phases in Figure 2 is determined by the condition $\tilde{\rho}_{xx} \approx \tilde{\rho}_{yy}$ or

$$\tilde{\sigma}_0 \approx 4\alpha^2 N^2\,. \tag{4}$$

hQHS phase. We show below that the hQHS phase resides between its upper border, Eq. (4), and its lower border $\tilde{\sigma}_0 \approx 3.5\,\alpha^2 N$, i.e., when

$$3.5\,\alpha^2 N \lesssim \tilde{\sigma}_0 \lesssim 4\alpha^2 N^2\,. \tag{5}$$

To find $\tilde{\rho}(N, \tilde{\sigma}_0)$, we start with Eqs. (38-39) of Ref. 15 [16],

$$\tilde{\sigma} = \frac{h v_F^2 g_B \tau_B}{2(1+\omega_c^2\tau_B^2)} = \frac{\tilde{\sigma}_0}{2(1+\omega_c^2\tau_B^2)}\,, \tag{6}$$

where

$$\frac{1}{\tau_B} \simeq \frac{1}{\tau}\frac{g_B}{g_0}\,. \tag{7}$$

Here, τ_B and g_B are the scattering time and the DOS at the center of the LL at $B \neq 0$, while v_F and $g_0 = m^\star/2\pi\hbar^2$ are the Fermi velocity and the DOS per spin at $B = 0$. [17]. Per Eq. (5), $\omega_c\tau_B = \omega_c\tau/\alpha = \tilde{\sigma}_0/2\alpha N \gg 1$ and Eq. (6) yields

$$\tilde{\sigma} \simeq \frac{2\alpha^2 N^2}{\tilde{\sigma}_0}\,. \tag{8}$$

Equation (5) also implies that $\tilde{\sigma} \ll \tilde{\sigma}_{xy} \simeq 2N$ and we find

$$\tilde{\rho} \simeq \frac{\tilde{\sigma}}{\tilde{\sigma}_{xy}^2} \simeq \frac{\alpha^2}{2\tilde{\sigma}_0}\,, \tag{9}$$

which coincides with Eq. (3). The independence of $\tilde{\rho}$ on N and its inverse proportionality to $\tilde{\sigma}_0$ are the hallmarks of the hQHS phase. At the end of this Rapid Communication we confirm this finding by calculating impurity scattering dominated σ_{xx} and σ_{yy} using a Kubo formula and being guided by Ref. 18.

AU phase. Using $\tilde{\sigma} = 2N/\pi$ calculated in Ref. 11 for low mobility samples with $\tau = \tau_{\rm q}$ and $\tilde{\sigma}_{xy} \simeq 2N$ we find

$$\tilde{\rho} = \frac{\tilde{\sigma}}{\tilde{\sigma}^2 + \tilde{\sigma}_{xy}^2} \simeq \frac{0.14}{N}\,. \tag{10}$$

This parameter-free result matches Eq. (9) at the upper border of the AU phase, $\tilde{\sigma}_0 = 3.5\,\alpha^2 N$, mentioned above and shown in Figure 2. This border can also be estimated by equating Γ_s and $\Gamma_i = \hbar\sqrt{2\omega_c/\pi\tau}$.

CZS phase. Using Eq. (6) with $g_B = g_0\sqrt{\omega_c\tau_{\rm q}} \gg 1$ [12, 19, 20], we find $\omega_c\tau_B = \sqrt{\omega_c\tau^2/\tau_{\rm q}} \gg 1$ and Eq. (6) gives

$$\tilde{\sigma} \simeq \frac{\tau_{\rm q}}{\tau} N\,, \tag{11}$$

which has an extra factor of $\pi\tau_{\rm q}/2\tau$ compared to $\tilde{\sigma} = 2N/\pi$ in the AU phase [11]. For $\tau_{\rm q}/\tau \ll 1$, we have $\tilde{\sigma} \ll \tilde{\sigma}_{xy}$ and

$$\tilde{\rho} \simeq \frac{\tilde{\sigma}}{\tilde{\sigma}_{xy}^2} = \frac{1}{4}\frac{\tau_{\rm q}}{\tau}\frac{1}{N}\,, \tag{12}$$

which agrees with Eq. (6) of Ref. 12. Equation (12) matches $\tilde{\rho}$ in the AU phase, Eq. (10), at $\tau \approx 1.7\,\tau_{\rm q}$ or at

$$\tilde{\sigma}_0 \approx 1.7\,\tilde{\sigma}_{\rm q}\,,\quad \tilde{\sigma}_{\rm q} \equiv \frac{hn_e\tau_{\rm q}}{m^\star}\,. \tag{13}$$

Equation (12) also matches $\tilde{\rho}$ in the hQHS phase, Eq. (9), at

$$N \approx N_{\rm q} \equiv \frac{\tilde{\sigma}_{\rm q}}{2\alpha^2} = \frac{hn_e\tau_{\rm q}}{2\alpha^2 m^\star}\,. \tag{14}$$

Let us now discuss predictions of our phase diagram (Figure 2) for $\tilde{\rho}(N)$ of three hypothetical samples with $\tilde{\sigma}_0 = 2\times10^3, 5\times10^3$ and 1×10^4, shown in Figure 3. The first sample resides in the AU phase at all N and obeys Eq. (10). The second one is in the hQHS phase at $N < 4$ and, therefore, its $\tilde{\rho}(N)$ is given by Eq. (9) and is independent on N. This plateau ends at $N \geq 4$, at which $\tilde{\rho}(N)$ starts declining as $1/N$ as prescribed by Eq. (10). Finally, the third sample shows anisotropic $\tilde{\rho}(N)$ at $N = 2$, then a plateau between $N = 3$ and $N = N_{\rm q} = 7$, and eventually follows Eq. (12) of the CZS phase at $N > 7$. If such a plateau is observed, one should be able to find $\tau_{\rm q}$ from experimental $N_{\rm q}$.

Above we considered a smectic phase pinned by disorder [8, 9]. If the disorder is able to create dislocations leading to a nematic phase, the conductivity of the hQHS phase will not be affected as it is sensitive only to the density of states. In the highest mobility sample of Figure 3, the anisotropic QHS phase happens at $\Gamma_i \ll \Gamma_s$ when dislocations are very sparse and, as a result, their effect on the electron drift along the stripe edges is negligible.

So far we dealt with very low temperatures T at which long-range stripe order is preserved. It is known, however, that at $T \gtrsim 0.1$ K the resistivity anisotropy vanishes while the local stripe order is believed to persist [21]. One can imagine this emerging phase as an ensemble of randomly oriented stripe domains [22–24]. The resistivity of such a 2D polycrystal

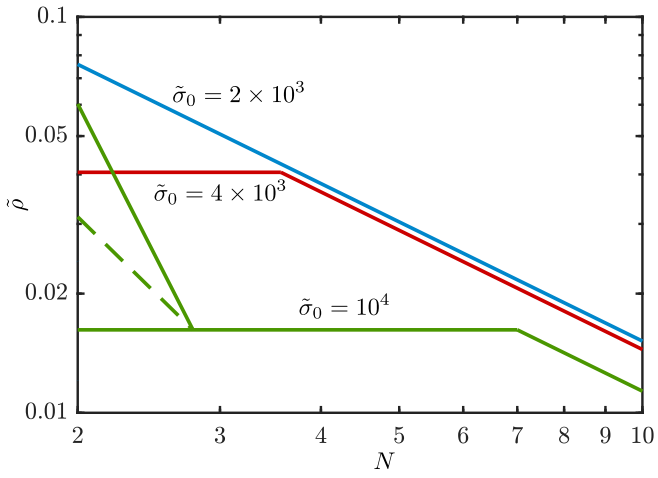

Figure 3. Predicted low-temperature $\tilde{\rho}$ for three hypothetical samples with $\tilde{\sigma}_0 = 2\times10^3, 4\times10^3$ and 1×10^4 (full lines). The resistivity of the conjectured polycrystal phase is shown by the dashed line.

is known [25] to be $\rho = (\rho_{xx}\rho_{yy})^{1/2}$. This means that the hQHS phase should not be affected, while in the QHS phase one expects isotropic $\tilde{\rho} \propto N^{-2}$ (see dashed line in Figure 3).

We next justify our use of the above semi-quantitative approach of Eq. (6). For a σ_{xx} due to short range impurity scattering the Kubo formula yields

$$\sigma_{xx} = \frac{\pi\hbar e^2}{L_x L_y}\sum_{i,j}\left\langle\left|\dot{X}_{ij}\right|^2\right\rangle\delta(E_F-\epsilon_i)\delta(E_F-\epsilon_j)\,, \tag{15}$$

where L_x and L_y are sample dimensions, E_F is the Fermi energy, i and j run over states with energies ϵ_i and ϵ_j, $X = -l_B^2 p_y/\hbar$ and $U(\mathbf{r}) = U_0 a^3\sum_l \delta^{(3)}(\mathbf{r}-\mathbf{r}_l)$ is the impurity potential with range of the lattice constant a. The electron wavefunction in the Landau gauge is given by

$$\psi_i(\mathbf{r}) = \phi(z)\exp\left(\frac{-iyX_i}{l_B^2}\right)\frac{\chi_N(x-X_i)}{\sqrt{L_y}}\,, \tag{16}$$

$$\chi_N(x) = \frac{\exp\left(-x^2/2l_B^2\right)H_N(x/l_B)}{\pi^{1/4}\sqrt{2^N N! l_B}}\,, \tag{17}$$

$$\phi(z) = (2/w)^{1/2}\sin(\pi z/w)\,, \tag{18}$$

where w is the width of the quantum well. The velocity matrix element can be written as $\dot{X}_{ij} = (i/\hbar)(X_j - X_i)U_{ij}$ and

$$\begin{aligned}\sigma_{xx} =& \frac{\pi e^2}{\hbar L_x L_y}\sum_{i,j}\left\langle|U_{ij}|^2\right\rangle(X_i-X_j)^2\\ &\times\delta(E_F-\epsilon_i)\delta(E_F-\epsilon_j)\,.\end{aligned} \tag{19}$$

For short range impurities with the 3D concentration N_3 and the correlator $\langle U(\mathbf{r})U(\mathbf{r}')\rangle = N_3(U_0a^3)^2\delta^{(3)}(\mathbf{r}-\mathbf{r}')$, we have

$$\begin{aligned}\left\langle|U_{ij}|^2\right\rangle &= \int \mathrm{d}\mathbf{r}\,\mathrm{d}\mathbf{r}'\,\psi_i^*(\mathbf{r})\psi_j(\mathbf{r})\psi_i(\mathbf{r}')\psi_j^*(\mathbf{r}')\,\langle U(\mathbf{r})U(\mathbf{r}')\rangle\\ &= \frac{3N_3(U_0a^3)^2}{2wL_y}\int \mathrm{d}x\,\chi_N^2(x-X_i)\chi_N^2(x-X_j)\,.\end{aligned} \tag{20}$$

Using $\delta(E_f-\epsilon_i)=\sum_m \delta(X_i-x^{(m)})/eE$ where $x^{(m)}$ is the m-th solution of $\epsilon(x)=V(x)=E_F$, $eE=|\mathrm{d}\epsilon/\mathrm{d}x|_{x=x^{(m)}}$, and $\sum_i=(L_y/2\pi l_B^2)\int \mathrm{d}X_i$, we arrive at

$$\sigma_{xx}=\frac{e^2 g_B^2 R_c^2}{2g_0\tau}\eta_x\,. \tag{21}$$

Here we have ignored all terms in the summation with $|X_i-X_j|>\Lambda/2$, as these terms are exponentially suppressed by the overlap of the wave functions in U_{ij}. Additionally, we have introduced the transport relaxation rate in zero magnetic field

$$\frac{1}{\tau}=\frac{2\pi}{\hbar}g_0\frac{3N_3(U_0a^3)^2}{2w}\,, \tag{22}$$

and a dimensionless coefficient

$$\eta_x=\left(\frac{\Lambda}{2R_c}\right)^2\Lambda\int \mathrm{d}x\,\chi_N^2(x)\chi_N^2(x-\Lambda/2)\,, \tag{23}$$

which oscillates with N and tends to 1.07 at $N\to\infty$. For $\Lambda=2.84\,R_c$ and $N>2$, $\eta_x(N)=1.07\pm0.15$. By equating σ_{xx}/g_Be^2 in Eq. (21) and D_{xx} given by Eqs. (2) and (7) of Ref. 9, we can now conclude that the coefficient γ entering Eq. (1), and used in Eqs. (2), (3), (4), is $\gamma\simeq\eta_x/2\simeq0.53$.

Similar to σ_{xx}, we can compute σ_{yy} as

$$\sigma_{yy}=\frac{\pi\hbar e^2}{L_xL_y}\sum_{i,j}\left\langle\left|\dot{Y}_{ij}\right|^2\right\rangle\delta(E_F-\epsilon_i)\delta(E_F-\epsilon_j)\,. \tag{24}$$

The velocity operator along $\hat{y}$ can be written as

$$\dot{Y}=\frac{i}{\hbar}[H,Y]=-\frac{l_B^2}{\hbar}\frac{\partial U}{\partial x}\,, \tag{25}$$

where we have ignored the drift in internal electric field $\mathbf{E}$ and used $Y=l_B^2p_x/\hbar$. The matrix element $\dot{Y}_{ij}$ can then be evaluated via integration by parts,

$$\dot{Y}_{ij}=\frac{l_B^2}{\hbar}\int \mathrm{d}\mathbf{r}\,U(\mathbf{r})\frac{\partial}{\partial x}[\psi_i^*(\mathbf{r})\psi_j(\mathbf{r})]\,. \tag{26}$$

After averaging over impurities positions,

$$\begin{aligned}\left\langle\left|\dot{Y}_{ij}\right|^2\right\rangle&=\frac{l_B^4}{\hbar^2}\frac{3N_3(U_0a^3)^2}{2wL_y}\\&\times\int \mathrm{d}x\left\{\frac{\mathrm{d}}{\mathrm{d}x}[\chi_N(x-X_i)\chi_N(x-X_j)]\right\}^2,\end{aligned} \tag{27}$$

we obtain

$$\begin{aligned}\sigma_{yy}&=\frac{\pi e^2}{\hbar L_x}\frac{l_B^4}{(2\pi l_B^2eE)^2}\int \mathrm{d}X_i\,\mathrm{d}X_j\,\frac{3N_3(U_0a^3)^2}{2w}\\&\times\int \mathrm{d}x\left\{\frac{\mathrm{d}}{\mathrm{d}x}[\chi_N(x-X_i)\chi_N(x-X_j)]\right\}^2\\&\times\sum_{m,n}\delta(X_i-x^{(m)})\delta(X_j-x^{(n)})=\frac{e^2g_B^2R_c^2}{2g_0\tau}\eta_y\,,\end{aligned} \tag{28}$$

where the summation of the product of delta functions can be evaluated separately for $m=n$ and for $m\neq n$. If $m=n$, then there are $2L_x/\Lambda$ terms with $X_i=X_j$. On the other hand, if $m\neq n$, there are $4L_x/\Lambda$ terms with $|X_i-X_j|=\Lambda/2$ (all other terms are negligible). This leads to η_y in Eq. (28),

$$\begin{aligned}\eta_y=\frac{\Lambda l_B^4}{2R_c^2}\int \mathrm{d}x\Bigg\{&\left[\frac{\mathrm{d}}{\mathrm{d}x}\left(\chi_N^2(x)\right)\right]^2\\&+2\left[\frac{\mathrm{d}}{\mathrm{d}x}(\chi_N(x)\chi_N(x-\Lambda/2))\right]^2\Bigg\}\,.\end{aligned} \tag{29}$$

For $\Lambda=2.84R_c$ and $N>2$, $\eta_y(N)=1.06\pm0.01$.

Using Eqs. (21), (28) we finally obtain dimensionless conductivities in the HQHS phase,

$$\tilde{\sigma}_{xx}=\frac{2\eta_x\alpha^2N^2}{\tilde{\sigma}_0},\quad \tilde{\sigma}_{yy}=\frac{2\eta_y\alpha^2N^2}{\tilde{\sigma}_0}\,, \tag{30}$$

confirming that the conductivity agrees with Eq. (8) within 15 %, thus justifying a semi-quantitative isotropic approach based on Eq. (6). Such a weak anisotropy is directly related to the period $\Lambda=2.84\,R_c$. We have found by varying Λ that at $N\to\infty$ the anisotropy vanishes when $\Lambda=2.82\,R_c$. Thus, it is indeed expected to be small at $\Lambda=2.84\,R_c$.

In summary, we have predicted the existence of an isotropically conducting (hidden) quantum Hall stripe phase. This phase is expected to reside in a finite range of nearly half-filled LLs, between the anisotropic quantum Hall stripe and isotropic liquid phases. The hallmarks of this new phase are the independence of the resistivity on the LL index and its inverse proportionality to the Drude resistivity at zero magnetic field. Although we focused on 2DEG in GaAs, the conjectured hQHS phase might be relevant to other realizations of 2DEG, such as, e.g., graphene, which might not exhibit conventional QHSs due to the lack of intrinsic orienting mechanism.

We thank I. Dmitriev, M. Fogler, and X. Fu for valuable discussions. Calculations by Y. H. and M. S. were supported primarily by the NSF through the University of Minnesota MRSEC under Award No. DMR-1420013. M. Z. acknowledges support from the U.S. Department of Energy, Office of Science, Basic Energy Sciences, under Award No. DE-SC0002567.

* Corresponding author: huan1756@umn.edu

[1] A. A. Koulakov, M. M. Fogler, and B. I. Shklovskii, Phys. Rev. Lett. **76**, 499 (1996).
[2] M. M. Fogler, A. A. Koulakov, and B. I. Shklovskii, Phys. Rev. B **54**, 1853 (1996).
[3] R. Moessner and J. T. Chalker, Phys. Rev. B **54**, 5006 (1996).
[4] C. Wexler and A. T. Dorsey, Phys. Rev. B **64**, 115312 (2001).
[5] E. H. Rezayi, F. D. M. Haldane, and K. Yang, Phys. Rev. Lett. **83**, 1219 (1999).

[6] M. P. Lilly, K. B. Cooper, J. P. Eisenstein, L. N. Pfeiffer, and K. W. West, Phys. Rev. Lett. **82**, 394 (1999).

[7] R. R. Du, D. C. Tsui, H. L. Stormer, L. N. Pfeiffer, K. W. Baldwin, and K. W. West, Solid State Commun. **109**, 389 (1999).

[8] A. H. MacDonald and M. P. A. Fisher, Phys. Rev. B **61**, 5724 (2000).

[9] M. Sammon, X. Fu, Y. Huang, M. A. Zudov, B. I. Shklovskii, G. C. Gardner, J. D. Watson, M. J. Manfra, K. W. Baldwin, L. N. Pfeiffer, and K. W. West, Phys. Rev. B **100**, 241303(R) (2019).

[10] We used Eqs. (13), (48), and (43) of Ref. 2 to find Γ_s and α at $r_s \simeq 1$, typical of GaAs samples.

[11] T. Ando and Y. Uemura, J. Phys. Soc. Jpn. **36**, 959 (1974).

[12] P. T. Coleridge, P. Zawadzki, and A. S. Sachrajda, Phys. Rev. B **49**, 10798 (1994).

[13] Here, we have chosen $N_q = 7$ which, for $n_e \simeq 3 \times 10^{11}$ cm^{-2}, $m^\star \simeq 0.06\, m_e$ [26–30], corresponds to $\tau_{\rm q} \simeq 10^2$ ps [31].

[14] G. C. Gardner, J. D. Watson, S. Mondal, N. Deng, G. A. Csáthy, and M. J. Manfra, Appl. Phys. Lett. **102**, 252103 (2013).

[15] I. A. Dmitriev, A. D. Mirlin, D. G. Polyakov, and M. A. Zudov, Rev. Mod. Phys. **84**, 1709 (2012).

[16] Our Eq. (6) has a factor $1/2$ compared to Eq. (39) of Ref. 15 because we deal with spin resolved LLs.

[17] Note that τ_B in this Rapid Communication is four times smaller than the one in Ref. 9.

[18] G. R. Aizin and V. A. Volkov, Sov. Phys. JETP **60**, 844 (1984).

[19] M. E. Raikh and T. V. Shahbazyan, Phys. Rev. B **47**, 1522 (1993).

[20] A. D. Mirlin, E. Altshuler, and P. Wölfle, Ann. Phys. **5**, 281 (1996).

[21] K. B. Cooper, M. P. Lilly, J. P. Eisenstein, L. N. Pfeiffer, and K. W. West, Phys. Rev. B **65**, 241313(R) (2002).

[22] K. B. Cooper, J. P. Eisenstein, L. N. Pfeiffer, and K. W. West, Phys. Rev. Lett. **92**, 026806 (2004).

[23] H. Zhu, G. Sambandamurthy, L. W. Engel, D. C. Tsui, L. N. Pfeiffer, and K. W. West, Phys. Rev. Lett. **102**, 136804 (2009).

[24] Q. Shi, M. A. Zudov, B. Friess, J. Smet, J. D. Watson, G. C. Gardner, and M. J. Manfra, Phys. Rev. B **95**, 161404(R) (2017).

[25] A. M. Dykhne and A. A. Snarskiĭ, JETP **102**, 475 (2006).

[26] P. Coleridge, M. Hayne, P. Zawadzki, and A. Sachrajda, Surf. Sci. **361**, 560 (1996).

[27] Y.-W. Tan, J. Zhu, H. L. Stormer, L. N. Pfeiffer, K. W. Baldwin, and K. W. West, Phys. Rev. Lett. **94**, 016405 (2005).

[28] A. T. Hatke, M. A. Zudov, J. D. Watson, M. J. Manfra, L. N. Pfeiffer, and K. W. West, Phys. Rev. B **87**, 161307(R) (2013).

[29] A. V. Shchepetilnikov, D. D. Frolov, Y. A. Nefyodov, I. V. Kukushkin, and S. Schmult, Phys. Rev. B **95**, 161305(R) (2017).

[30] X. Fu, Q. A. Ebner, Q. Shi, M. A. Zudov, Q. Qian, J. D. Watson, and M. J. Manfra, Phys. Rev. B **95**, 235415 (2017).

[31] Q. Shi, M. A. Zudov, I. A. Dmitriev, K. W. Baldwin, L. N. Pfeiffer, and K. W. West, Phys. Rev. B **95**, 041403(R) (2017).